Published in final edited form as:
Anat Rec (Hoboken). 2010 May ; 293(5): 849–857. doi:10.1002/ar.21110.

Inflammation-Induced Intussusceptive Angiogenesis in Murine Colitis

Moritz A. Konerding[1], **Aslihan Turhan**[2], **Dino J. Ravnic**[2], **Miao Lin**[2], **Christine Fuchs**[1], **Timothy W. Secomb**[3], **Akira Tsuda**[4], and **Steven J. Mentzer**[2,*]

[1]Institute of Anatomy and Cell Biology, University Medical Center, Johannes Gutenberg-University, Mainz, Germany

[2]Laboratory of Adaptive and Regenerative Biology, Brigham and Women's Hospital, Harvard Medical School, Boston, Massachusetts

[3]Department of Physiology, University of Arizona, Tucson, Arizona

[4]Molecular and Integrative Physiological Sciences, Harvard School of Public Health, Boston, Massachusetts

Abstract

Intussusceptive angiogenesis is a morphogenetic process that forms new blood vessels by the division of a single blood vessel into two lumens. Here, we show that this process of intraluminal division participates in the inflammation-induced neovascularization associated with chemically induced murine colitis. In studies of both acute (4–7 days) and chronic (28–31 days) colitis, intravital microscopy of intravascular tracers demonstrated a twofold reduction in blood flow velocity. In the acute colitis model, the decreased velocity was associated with marked dilatation of the mucosal plexus. In contrast, chronic inflammation was associated with normal caliber vessels and duplication (and triplication) of the quasi-polygonal mucosal plexus. Scanning electron microscopy (SEM) of intravascular corrosion casts suggested that pillar formation and septation, previously linked to the morphogenetic process of intussusceptive angiogenesis, were present within days of the onset of inflammation. Four weeks after the onset of inflammation, SEM of vascular corrosion casts demonstrated replication of the mucosal plexus without significant evidence of sprouting angiogenesis. These data suggest that mucosal capillaries have comparable aggregate cross-sectional area in acute and chronic colitis; however, there is a significant increase in functional capillary density in chronic colitis. We conclude that intussusceptive angiogenesis is a fundamental mechanism of microvascular adaptation to prolonged inflammation.

Keywords

angiogenesis; corrosion casting; intravital microscopy; microcirculation; scanning electron microscopy

The microvascular adaptations to local inflammation depend upon the structure of the preexisting capillary reserve. In skeletal muscle, the increased metabolic demand of exercise or inflammation results in a rapid threefold increase in the number of perfused capillaries (Chambers and Zweifach, 1942; Clark and Clark, 1943; Honig et al., 1980). In the mouse

*Correspondence to: Dr. Steven J. Mentzer, Room 259, Division of Thoracic Surgery, Brigham and Women's Hospital, 75 Francis Street, Boston, MA 02115. Fax: +617-730-2898. smentzer@partners.org.

ear, acute inflammation stimulates a similar increase in functional capillary density (Ravnic et al., 2006a). In these tissues, preexisting capillaries can be recruited to increase functional capillary density. In contrast, tissues such as the colon do not have a preexisting capillary reserve; nonetheless, prolonged inflammatory conditions appear to result in increased vascularity (Erikson et al., 1970; Hulten et al., 1977; Kruschewski et al., 1995). These observations suggest that mechanisms distinct from blood flow regulation may be capable of increasing the number of capillaries in chronically inflamed tissues.

Attempts to define the structural adaptations in the inflammatory microcirculation have focused on changes occurring within days of the application of antigen. In the sheep skin, the application of epicutaneous antigen resulted in the focal dilatation of dermal capillary loops (Secomb et al., 2003). The acute dilatation—termed microangiectasias—was associated with focally diminished flow velocity and lymphocyte transmigration (West et al., 2001; Secomb et al., 2003). In a murine colitis model, chemically induced inflammation produced acute dilatation of the mucosal plexus (Ravnic et al., 2007a). Similar to observations in the skin, the dilatation was associated with decreased flow velocity and lymphocyte transmigration (Ravnic et al., 2007a). Despite the relevance for human colitis, little is known about the structural changes of the capillaries exposed to prolonged inflammation of the colon.

In this report, we defined the structural and functional adaptations of the adult mouse colon to prolonged inflammation. The previously observed dilatation of the mucosal plexus within 7 days of the onset of inflammation was associated with signs of intussusceptive (nonsprouting) angiogenesis: namely, endothelial activation and pillar formation at vessel bifurcations. This process of intussusceptive angiogenesis led to duplication and triplication (and occasional quadruplication) of the mucosal plexus within 28–31 days. We conclude that intussusceptive angiogenesis is a fundamental mechanism of microvascular adaptation to prolonged inflammation.

Materials and Methods

Mice

Balb/c or C57B/6 mice (Jackson Laboratory, Bar Harbor, ME), 25–33 g, were used in all experiments. The care of the animals was consistent with guidelines of the American Association for Accreditation of Laboratory Animal Care (Bethesda, MD).

TNBS Administration

The colitis model was based on previous work (Elson et al., 1996; Neurath et al., 2000). After the mouse abdomen was sheared and cleansed with water, 36 μL of a 2.5% 2,4,6-trinitrochlorobenzene (TNCB) (ChemArt, Egling, Germany) in a 4:1 acetone/olive oil solution was sprayed onto a 1.5-cm diameter circular PhastTansfer Filter Paper (Pharmacia, Upsala, Sweden). The TNCB-soaked filter paper was applied to the sheared abdomen and secured with Tegaderm (3 M, St. Paul, MN) and Durapore Surgical Tape (3 M, St. Paul, MN). The TNCB patch was removed 24 hr after application. Six days later, 125 μL of a 1.75% 2,4,6-trinitrobenzenesulfonic acid (TNBS) (Sigma, St. Louis, MO) in a 50% ethanol solution was instilled into the rectum (Day 0) and weekly thereafter. Control mice had an identical volume of PBS instilled intrarectally. Acute inflammation was defined as the first week after stimulation. Chronic inflammation was defined as 28–31 days after the first stimulation.

Dextran Sulfate Administration

In C57/B6 mice, the dextran sodium sulfate (DSS) (TdB Consultancy AB, Uppsala, Sweden) model of colitis was similar to that described previously (Okayasu et al., 1990; Dieleman et al., 1998). Briefly, DSS was freshly prepared and added daily to the C57/B6 mice drinking water at a final concentration of 5%. The mice were assessed daily for clinical signs and total body weight. The DSS treatment was continued for 5 days and then changed to water for the remainder of the experimental period.

Intravital Microscopy System

The exteriorized tissue was imaged using a Nikon Eclipse TE2000 inverted epifluorescence microscope using Nikon water dipping objectives of 10×, 20×, 40×, and 60× linear magnification with fluorite, flat field, and infinity correction. An X-Cite (Exfo; Vanier, Canada) 120 W metal halide light source and a liquid light guide were used to illuminate the tissue samples. Excitation and emission filters (Chroma, Rockingham, VT) in separate LEP-motorized filter wheels were controlled by a MAC5000 controller (Ludl, Hawthorne, NY) and MetaMorph software 7.01 (Molecular Devices). The 14-bit fluorescent images were digitally recorded on a C9100-02 camera (Hamamatsu, Japan). The C9100-02 has a hermetic vacuum-sealed air-cooled head and on-chip electron gain multiplication (2,000×). Images with 1,000 × 1,000 pixel resolution were routinely obtained at 50 fps; frame rates exceeding 100 fps were routinely obtained with binning and subarrays. The images were recorded in image stacks comprising 30 sec to 10 min video sequences.

Nanoparticles

Fluorescent nanoparticles were developed by Molecular Probes (Invitrogen, Eugene, OR) for intravascular particle tracking (Ravnic et al., 2007b). These particles have superior fluorescent characteristics, small size (200–500 nm) and low surface charge content (6.2 μEq/g). The nanoparticles used in this study were green (ex 488; em 510) and infra-red (ex 655 nm; em 710 nm).

Intravital Fluorescence Labeling

A 5-(and −6)-carboxyfluorescein diacetate succinimidyl ester (CFSE) (Molecular Probes, Eugene, OR) labeling solution was prepared in DMSO as described (Becker et al., 2004). The freshly prepared CFSE (400 μL) was intravenously injected over 2–3 min. The CFSE tracer (ex 480 nm, em 520 nm) was imaged with 25-nm bandpass filters (Omega).

Multiframe Particle Tracking

Particle tracking was performed on digitally recorded and distance calibrated multiimage “stacks”(Ravnic et al., 2006b). The image stacks produced a sequential time history of velocity and direction as the acquired images were time stamped based on the 100 MHz system bus clock of the Xeon processor (Intel, Santa Clara, CA). The movement of individual particles was tracked using the MetaMorph (Molecular Devices) object tracking applications. The intensity centroids of the particles were identified and their displacements tracked through planes in the source image stack. For displacement reference, the algorithm used the location of the particle at its first position in the track. Each particle was imaged as a high contrast fluorescent disk and its position was determined with subpixel accuracy. The image of the particle was tracked using a cross-correlation centroid-finding algorithm to determine the best match of the particle/cell position in successive images. With routine distance calibration, the overlay of the image stack provides a quantitative assessment of the particle/cell path and mean particle velocity.

Time-Series Angiogram

Image stacks of fluorescent nanoparticle passage through the mucosal plexus were processed to produce a time-series angiogram. For each image stack, a maximum filter was used to identify the maximum pixel intensity value for all the pixels at that position. Because the fluorescent nanoparticles provided a high contrast disk relative to background, the resultant image provided a high contrast angiogram reflecting nanoparticle flow paths. Time-series angiograms were used to confirm particle tracking velocity measurements.

Scanning Electron Microscopy

After systemic heparinization with 750 U of heparin per kg i.v., the mice were thoracotomized in deep anesthesia. The aorta was cannulated through the left ventricle with an olive-tipped cannula and perfused with 15–20 mL of 37°C saline followed by a buffered 2.5% glutaraldehyde solution (Sigma) at pH 7.40. After casting of the microcirculation with 15 mL of Mercox (SPI, West Chester, PA) diluted with 20% methylmethacrylate monomers (Aldrich) and caustic digestion, the microvascular corrosion casts were imaged after coating with gold in an argon atmosphere with a Philips ESEM XL30 scanning electron microscope. Stereopair images were obtained by using tilt angles from 6° to 20°. The quality of the filling of the corrosion casts was also checked by comparisons with the vascular densities in semithin light microscopic sections stained with methylene blue. The corrosion casts demonstrated filling of the whole capillary bed from artery to vein without evidence of extravasation or pressure distension.

Statistical Analysis

The statistical analysis was based on measurements from a minimum of three different mice at each time point. The unpaired Student *t* test for samples of unequal variances was used to calculate statistical significance. The data were expressed as mean ± 1 standard deviation. The significance level for the sample distribution was defined as $P < 0.01$.

Results

Chemically Induced Colitis

Consistent with previous reports (Neurath et al., 2000), the repeated rectal instillation of TNBS in presensitized mice produced a model of chronic inflammatory colitis. Rectal instillation of TNBS was repeated weekly for 4 weeks. Clinical signs of inflammation, such as decreased activity (78%) and ruffled fur (56%), were present in most of the mice after the first challenge but became less apparent with repeated TNBS challenges. Total body weight, reflecting acute inflammation-associated obstipation, declined for 4–5 days but gradually returned to near-control levels (Fig. 1A). Although the surviving mice appeared to adapt to the repeated instillation of TNBS, there was 40% mortality within the first 14 days (Fig. 1B). In DSS-induced colitis, oral administration of DSS was continued for 5 days followed by water alone for the remainder of the experimental period. Clinical signs of colitis were less prominent, and total body weight decline was less severe than in TNBS-induced colitis (Fig. 1C). Mortality within the first 14 days was <10% (Fig. 1D).

Diminished Flow Velocity

The effect of prolonged inflammation on blood flow velocity was investigated by tracking intravenously injected fluorescent nanoparticles by epifluorescence intravital videomicroscopy. Confirming previous work (Ravnic et al., 2007a), blood flow velocity measured 4–7 days after the initial challenge was significantly lower velocity in the inflamed microcirculation (mean ± SD, 710 ± 479 μm/sec; N = 12) than in the normal mucosal plexus (mean ± SD, 1593 ± 798 μm/sec; N = 12) ($P < 0.001$) (Fig. 2A). Given the

clinical improvement in the mice, an unexpected finding was that the chronically stimulated mice, 26–33 days after the initial antigen challenge, continued to demonstrate reduced blood flow velocity. The mice repeatedly challenged with TNBS had a lower mean blood flow velocity (659 ± 456 μm/sec; N = 8) than mice challenged with a PBS control vehicle (2056 ± 1106 μm/sec; N = 6) ($P < 0.001$) (Fig. 2A). Similarly, mice with DSS-induced colitis had a lower mean blood flow velocity in both acute (DSS 1140 ± 719 μm/sec, N = 8; control 2172 ± 1178 μm/sec, N = 6) and chronic (DSS 1309 ± 7101 μm/sec, N = 8; control 2261 ± 788 μm/sec, N = 6) than mice treated with water alone (Fig. 2B).

Inflammation-Induced Neovascularization

The prolonged decrease in flow velocity in the mucosal plexus suggested that structural adaptations might contribute to both the clinical 28–31 days after the onset of inflammation were examined by tilt-angle SEM. SEM demonstrated regions of the mucosa with replication of the superficial vascular plexus. Some regions of the mucosa demonstrated duplication, triplication, and even quadruplication of the vascular plexus (Fig. 3). The distribution of the replicated vessels appeared to correspond to previously defined flow regions of the mucosal plexus (Turhan et al., 2007); some regions demonstrated extensive replication of the superficial plexus, whereas other regions demonstrated relatively little evidence of angiogenesis. Also observed were regional differences in the completeness of casting medium perfusion—possibly because of platelet aggregates in the inflammatory mucosal plexus (Miele et al., 2009). Because of this variability, a comprehensive statistical assessment of the prevalence of vessel replication was not possible; however, the statistical comparison of completely casted flow regions with vessel replication and randomly selected regions from control mice demonstrated a significant increase in vascular density ($P < 0.001$; Fig. 4).

Mechanism of Replication

To investigate the mechanism of vessel replication, corrosion casting and SEM were performed of the mucosal plexus 4–7 days after the onset of inflammation. In both DSS- and TNBS-induced colitis, small holes were observed within the corrosion casts at the vessel bifurcations (Fig. 5: A,B,C, TNBS; D,E,F, DSS). The constant morphology and nonrandom distribution of these holes suggested a process of pillar formation previously observed in the developing rat lung (Caduff et al., 1986;Burri and Tarek, 1990) and chick chorioallantoic membrane (Patan et al., 1993); namely, intussusceptive (nonsprouting) angiogenesis. The presence of pillar formation and the associated endothelial activation was investigated by TEM. TEM of the mucosal plexus vessels 6 days after the onset of DSS-induced inflammation demonstrated ultrastructural changes consistent with endothelial activation and endothelial folds separating the vessel lumens (Fig. 6A–D). The presence of collagen fibers within the luminal pillar also suggests the participation of nonendothelial cells in pillar formation (Fig. 6D).

Discussion

In this report, we studied the microvascular adaptations associated with prolonged inflammation in murine colitis. In both TNBS and DSS models of colitis, chronic inflammation resulted in either unremitting clinical decline or resolution of the initial weight loss and the return of baseline activity levels. In surviving mice, intravital microscopy demonstrated diminished mean blood flow velocities that were comparable to velocities measured in acute colitis. Corrosion casting and SEM performed 28–31 days after the onset of inflammation demonstrated duplication and triplication of the mucosal plexus. Corrosion casting and SEM performed 4–7 days after the onset of inflammation demonstrated filling defects consistent with intussusceptive pillars. Pillars are a characteristic features of the

morphogenetic process of intussusceptive angiogenesis (Patan et al., 1996a). TEM confirmed endothelial activation and intraluminal pillar formation. We conclude that intussusceptive angiogenesis is a mechanism of inflammation-induced neovascularization in murine colitis.

Intussusceptive (nonsprouting) angiogenesis is a well-characterized morphogenetic process in the capillaries of the lung (Caduff et al., 1986; Burri and Tarek, 1990) and chorioallantoic membrane (Patan et al., 1993). Intussusceptive angiogenesis is a process of intravascular septation that produces two lumens from a single vessel (Patan et al., 1996a). Alternatively, a preexisting bifurcation can be remodeled by similar process (Djonov et al., 2003). In both cases, pillars bridge the opposing sides of the microvessel lumen. The bridging pillars produce a characteristic “hole” in the corrosion cast of the vessel lumen. In morphogenetic studies, the pillar is initially formed by a zone of endothelial contact. The endothelial bridge develops into a pillar containing myofibroblasts and pericytes (Burri et al., 2004). This process appears to be regulated, at least in part, by microhemodynamic forces (Djonov et al., 2002; Kurz et al., 2003) and eventually leads to remodeling and separation of the capillary into two capillaries.

Intussusceptive angiogenesis is distinct from sprouting angiogenesis because it (1) has no necessary requirement for cell proliferation, (2) can rapidly expand an existing capillary network, and (3) can maintain organ function during replication (Patan et al., 1992; Folkman and D'Amore, 1996; Burri and Djonov, 2002). In the murine colitis model, holes in the corrosion casts were observed within 4–7 days, and replication of the entire mucosal plexus occurred within 4 weeks. This rapid adaptation likely contributed to the survival of the 60% of the mice living beyond 14 days in the TNBS model. In contrast to skin or muscle, the colon mucosal plexus has no apparent precapillary-like sphincter activity (Turhan et al., 2007) and no obvious capillary reserve. In the absence of a recruitable capillary reserve, intussusceptive angiogenesis appears to be a critical adaptation for meeting the metabolic demands of prolonged inflammation.

Intussusceptive angiogenesis is a process of microvascular expansion that has now been described in morphogenesis (Schlatter et al., 1997), tumorigenesis (Patan et al., 1996b), and chronic inflammation. Intussusceptive or nonsprouting angiogenesis provides a mechanism for the expansion of an existing microvascular network; sprouting angiogenesis provides a mechanism for expanding microvessels in tissues without a preexisting network. In our electron microscopy studies, both processes involve morphologic similarities. In particular, the ultrastructural appearance of the activated endothelial cells is remarkably similar in both sprouting and nonsprouting angiogenesis. We speculate that the participating angiogenic mediators are similar in both processes. Perhaps, the orientation of endothelial cell migration —extraluminal migration in sprouting angiogenesis and intraluminal migration in nonsprouting angiogenesis—reflects the fundamental distinction between these processes.

An interesting functional observation was the similar blood flow velocity in the acute and chronic colitis conditions. The comparable blood flow velocity may reflect a similar aggregate cross-sectional area of the acutely and chronically inflamed mucosal plexus. In colonic inflammation, the mucosal plexus dilates in the acute phase and replicates in the chronic phase. Although the cross-sectional area was likely similar, the functional capillary density (Mathieu-Costello et al., 1995) was significantly different. In acute inflammation, the number of capillaries containing red blood cells in a defined area of the mucosal plexus was the same as the PBS controls. In prolonged inflammation, the average number of perfused capillaries increased two- to threefold. When compared with simple dilatation, an adaptive advantage of capillary replication is the significant increase in the exchange surface area.

A potential reason that intussusceptive angiogenesis has not been previously suspected as a response to inflammation is the difficulty in recognizing plexus replication in two-dimensional tissue sections. Although increased vascularity has been noted in chronic colitis (Erikson et al., 1970; Hulten et al., 1977; Kruschewski et al., 1995), the identification of structural adaptations requires corrosion casting and SEM. Moreover, there is no reliable immunohistochemical or cytomorphologic marker for the process of intussusceptive angiogenesis. The pillar and septal formation of intussusceptive angiogenesis is currently only identified by corrosion castings and SEM.

In summary, intussusceptive angiogenesis appears to be a fundamental mechanism of microvascular adaptation to prolonged inflammatory colitis. The septation process in the mucosal plexus provides an effective adaptation for rapidly increasing both the capillary density and the exchange surface area of the mucosal plexus. The adaptive advantage of rapidly increasing capillary exchange surface area may be equally relevant in inflammatory and ischemic conditions. Further, we speculate that intussusceptive angiogenesis may be a relevant process in a variety of tissues. The participation of intussusceptive angiogenesis in human disease as well as the cellular and molecular control of the process of intussusceptive angiogenesis is an important question for future studies.

Acknowledgments

Grant sponsor: NIH; Grant numbers: HL47078, HL75426, HL94567.

Literature Cited

Becker HM, Chen M, Hay JB, Cybulsky MI. Tracking of leukocyte recruitment into tissues of mice by in situ labeling of blood cells with the fluorescent dye CFDA SE. J Immunol Methods 2004;286:69–78. [PubMed: 15087222]

Burri PH, Djonov V. Intussusceptive angiogenesis—the alternative to capillary sprouting. Mol Aspects Med 2002;23:S1–S27. [PubMed: 12537983]

Burri PH, Hlushchuk R, Djonov V. Intussusceptive angiogenesis: its emergence, its characteristics, and its significance. Dev Dyn 2004;231:474–488. [PubMed: 15376313]

Burri PH, Tarek MR. A novel mechanism of capillary growth in the rat pulmonary microcirculation. Anat Rec 1990;228:35–45. [PubMed: 2240600]

Caduff JH, Fischer LC, Burri PH. Scanning electron microscope study of the developing microvasculature in the postnatal rat lung. Anat Rec 1986;216:154–164. [PubMed: 3777448]

Chambers R, Zweifach BW. Caliber changes of the vessels of the capillary bed. Fed Am Soc Exp Biol 1942;1:14.

Clark ER, Clark EC. Caliber changes in minute blood vessels observed in the living mammal. Am J Anat 1943;73:215–250.

Dieleman LA, Palmen MJ, Akol H, Bloemena E, Pena AS, Meuwissen SG, Van Rees EP. Chronic experimental colitis induced by dextran sulphate sodium (DSS) is characterized by Th1 and Th2 cytokines. Clin Exp Immunol 1998;114:385–391. [PubMed: 9844047]

Djonov V, Baum O, Burri PH. Vascular remodeling by intussusceptive angiogenesis. Cell Tissue Res 2003;314:107–117. [PubMed: 14574551]

Djonov VG, Kurz H, Burri PH. Optimality in the developing vascular system: branching remodeling by means of intussusception as an efficient adaptation mechanism. Dev Dyn 2002;224:391–402. [PubMed: 12203731]

Elson CO, Beagley KW, Sharmanov AT, Fujihashi K, Kiyono H, Tennyson GS, Cong Y, Black CA, Ridwan BW, McGhee JR. Hapten-induced model of murine inflammatory bowel disease: mucosa immune responses and protection by tolerance. J Immunol 1996;157:2174–2185. [PubMed: 8757344]

Erikson U, Fagerberg S, Krause U, Olding L. Angiographic studies in Crohn's disease and ulcerative colitis. Am J Roentgenol Radium Ther Nucl Med 1970;110:385–392.

Folkman J, D'Amore PA. Blood vessel formation: what is its molecular basis? Cell 1996;87:1153–1155. [PubMed: 8980221]

Honig CR, Odoroff CL, Frierson JL. Capillary recruitment in exercise: rate, extent, uniformity, and relation to blood flow. Am J Physiol 1980;238:H31–H42. [PubMed: 7356032]

Hulten L, Lindhagen J, Lundgren O, Fasth S, Ahren C. Regional intestinal blood flow in ulcerative colitis and Crohn's disease. Gastroenterology 1977;72:388–396. [PubMed: 832785]

Kruschewski M, Busch C, Dorner A, Lierse W. Angio-architecture of the colon in Crohn disease and ulcerative colitis. Light microscopy and scanning electron microscopy studies with reference to the morphology of the healthy large intestine. Langenbecks Arch Chir 1995;380:253–259. [PubMed: 7500795]

Kurz H, Burri PH, Djonov VG. Angiogenesis and vascular remodeling by intussusception: from form to function. News Physiol Sci 2003;18:65–70. [PubMed: 12644622]

Mathieu-Costello O, Manciet LH, Tyml K. Capillary ultrastructure and functional capillary density. Int J Microcirc Clin Exp 1995;15:231–237. [PubMed: 8852620]

Miele LF, Turhan A, Lee GS, Lin M, Ravnic DJ, Tsuda A, Konerding MA, Mentzer SJ. Blood flow patterns spatially associated with platelet aggregates in murine colitis. Anat Rec 2009;292:1143–1153.

Neurath M, Fuss I, Strober W. TNBS-colitis. Int Rev Immunol 2000;19:51–62. [PubMed: 10723677]

Okayasu I, Hatakeyama S, Yamada M, Ohkusa T, Inagaki Y, Nakaya R. A novel method in the induction of reliable experimental acute and chronic ulcerative colitis in mice. Gastroenterology 1990;98:694–702. [PubMed: 1688816]

Patan S, Alvarez MJ, Schittny JC, Burri PH. Intussusceptive microvascular growth: a common alternative to capillary sprouting. Arch Histol Cytol 1992;55(Suppl):65–75. [PubMed: 1290678]

Patan S, Haenni B, Burri PH. Evidence for intussusceptive capillary growth in the chicken chorio-allantoic membrane (CAM). Anat Embryol (Berl) 1993;187:121–130. [PubMed: 8238959]

Patan S, Haenni B, Burri PH. Implementation of intussusceptive microvascular growth in the chicken chorioallantoic membrane (CAM). I. Pillar formation by folding of the capillary wall. Microvasc Res 1996a;51:80–98. [PubMed: 8812761]

Patan S, Munn LL, Jain RK. Intussusceptive microvascular growth in a human colon adenocarcinoma xenograft: a novel mechanism of tumor angiogenesis. Microvasc Res 1996b;51:260–272. [PubMed: 8778579]

Ravnic DJ, Konerding MA, Pratt JP, Wolloscheck T, Huss HT, Mentzer SJ. Inflammation-responsive focal constrictors in the mouse ear microcirculation. J Anat 2006a;209:807–816. [PubMed: 17118067]

Ravnic DJ, Konerding MA, Tsuda A, Jiang X, Huss HT, Pratt JP, Mentzer SJ. Structural adaptations in the murine colon microcirculation associated with hapten-induced inflammation. Gut 2007a; 56:518–523. [PubMed: 17114297]

Ravnic DJ, Tsuda A, Turhan A, Zhang YZ, Pratt JP, Huss HT, Mentzer SJ. Multi-frame particle tracking in intravital imaging: defining Lagrangian coordinates in the microcirculation. BioTechniques 2006b;41:597–601. [PubMed: 17140117]

Ravnic DJ, Zhang YZ, Turhan A, Tsuda A, Pratt JP, Huss HT, Mentzer SJ. Biological and optical properties of fluorescent nanoparticles developed for intravascular imaging. Microsc Res Tech 2007b;70:776–781. [PubMed: 17576122]

Schlatter P, Konig MF, Karlsson LM, Burri PH. Quantitative study of intussusceptive capillary growth in the chorioallantoic membrane (CAM) of the chicken embryo. Microvasc Res 1997;54:65–73. [PubMed: 9245646]

Secomb TW, Konerding MA, West CA, Su M, Young AJ, Mentzer SJ. Microangioectasias: structural regulators of lymphocyte transmigration. Proc Natl Acad Sci USA 2003;100:7231–7234. [PubMed: 12782790]

Turhan A, Konerding MA, Tsuda A, Ravnic DJ, Hanidizar D, Lin MY, Mentzer SJ. Bridging mucosal vessels associated with rhythmically oscillating blood flow in murine colitis. Anat Rec 2007;291:74–92.

West CA, He C, Su M, Secomb TW, Konerding MA, Young AJ, Mentzer SJ. Focal topographic changes in inflammatory microcirculation associated with lymphocyte slowing and transmigration. Am J Physiol Heart Circ Physiol 2001;281:H1742–H1750. [PubMed: 11557566]

Abbreviations used

DSS	dextran sodium sulfate
SEM	scanning electron microscopy
TEM	transmission electron microscopy
TNBS	2,4,6-trinitrobenzenesulfonic acid

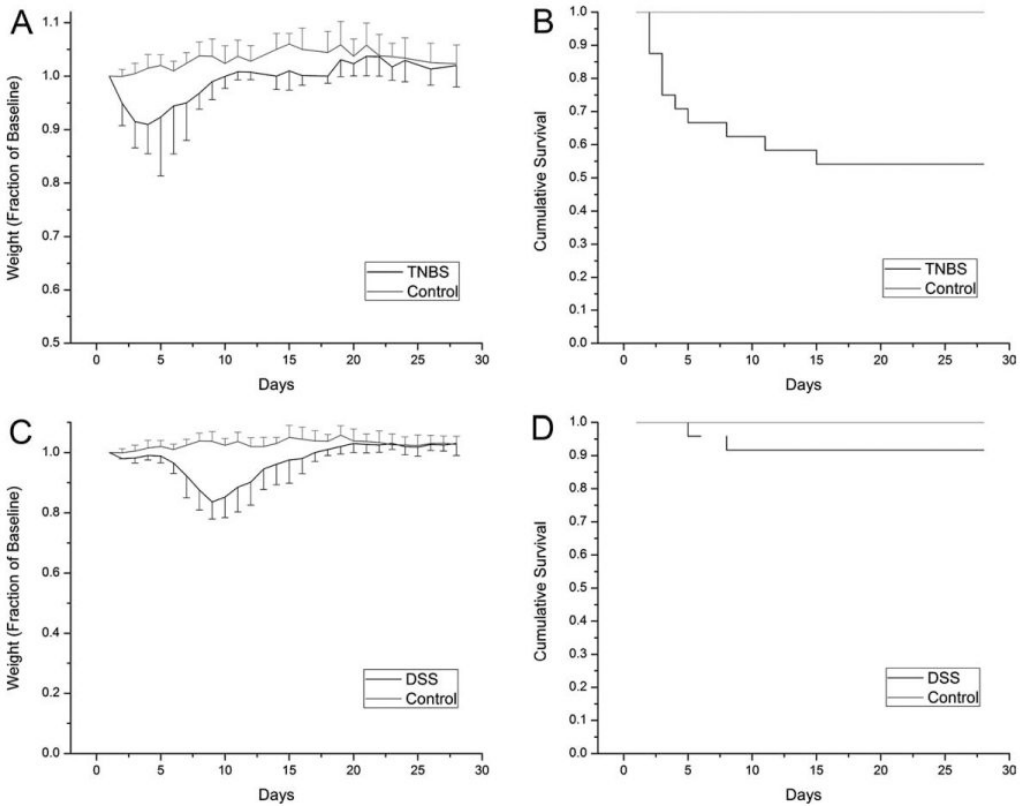

Fig. 1.

The time course of chemically induced colitis reflected by (**A, C**) changes in total body weight and (**B, D**) cumulative survival. The TNBS treated mice (N = 24) were challenged at weekly intervals after the initial challenge on Day 0. Control mice (N = 12) were treated in parallel with an equivalent volume of PBS. The DSS mice (N = 24) were treated with 2% DSS in the drinking water for 5 days followed by water alone for the remainder of the experimental period. The weight of the mice was expressed as a percentage of their baseline body weight (grams). The mice were carefully observed and euthanized if there was an unremitting decline in activity level or body weight. Error bars reflect 1 standard deviation.

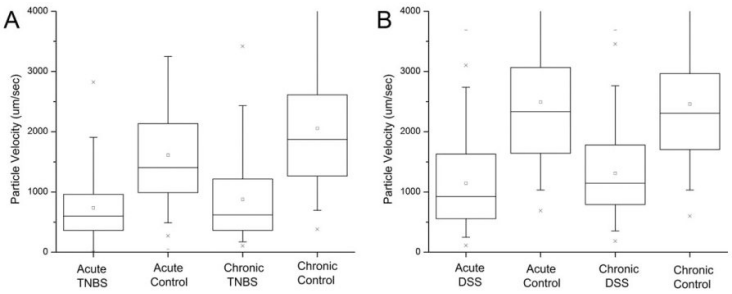

Fig. 2.

Flow velocity in the mucosal plexus during acute (4 days) and chronic (4 weeks) chemically induced colitis. Intravital videomicroscopy of fluorescent nanoparticles was used to define the velocity fields in acute colitis (TNBS N = 8; DSS N = 8) and controls (TNBS N = 8; DSS N = 8) mice as well as chronic colitis (TNBS N = 8; DSS N = 8) and controls (TNBS N = 8; DSS N = 8). (**A**) In the TNBS model, chronic colitis was defined as mice challenged with intrarectal TNBS at weekly intervals; control mice were treated with intrarectal PBS in parallel. (**B**) In the DSS model, the mice were treated with 2% DSS for 5 days followed by water alone. The velocities were measured at randomly selected regions of the mucosal plexus. The box chart shows the 25–75 percentile with 10th and 90th percentile delineated by error bars.

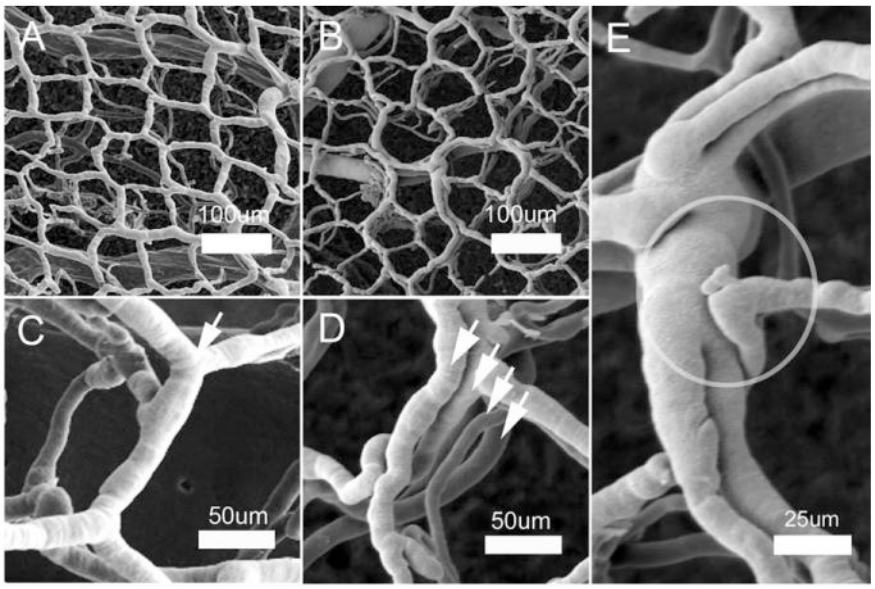

Fig. 3.

Corrosion casting and SEM of the mucosal plexus 28 days after the onset of treatment in TNBS-induced colitis. SEM of control (**A, C**) and colitis (**B–E**) demonstrated preservation of the polygonal configuration surrounding the mucosal crypts. In the chemically induced colitis, the mucosal plexus demonstrates replication of the plexus. High-resolution SEM (C, control; **D**, colitis) demonstrates replication of the plexus (arrows). (E) A dilated mucosal plexus vessel with apparent proximal and distal luminal division is shown. A structural feature, consistent with an angiogenic sprout, is also circled.

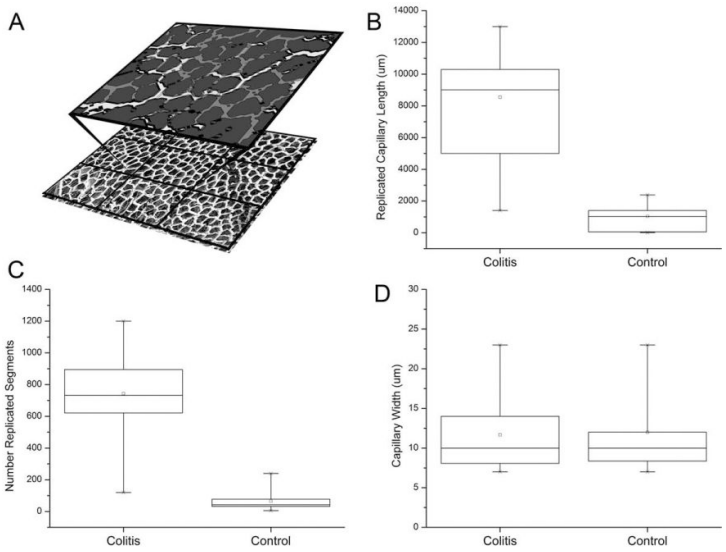

Fig. 4.

Morphometry and spatial statistical analysis demonstrated a significant increase in microvessel density and functional capillary length of mucosal plexus vessels 28–31 days after the onset of treatment (N = 6). (**A**) A reference grid was superimposed on corrosion casts of the mucosal plexus. Flow regions, defined by feeding arterioles and draining marginal veins (28), were compared in colitis (TNBS N = 3 mice; DSS N = 3 mice) and control (N = 3) mice. Within each flow region, the casts were segmented (A) and morphometrically analyzed. Both the total length (**B**) and number (**C**) of replicated segments were significantly greater in the colitis mice ($P > 0.001$). In contrast, there was no difference in vessel morphology as reflected by vessel diameter ($P > 0.05$) (**D**). The box chart shows the 25–75 percentile with 10th and 90th percentile delineated by error bars.

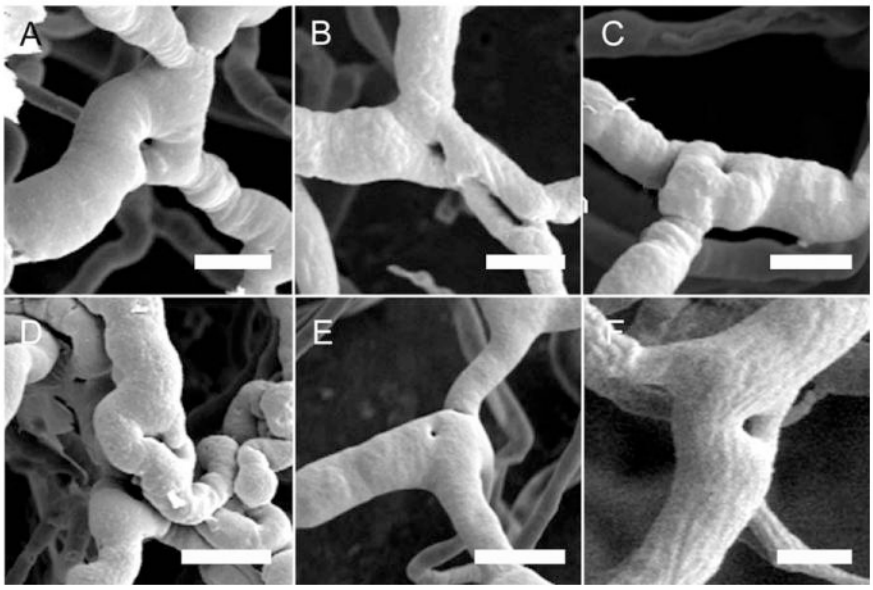

Fig. 5.

Scanning electron micrographs of corrosion casts in mice 4–7 days after the onset of treatment (**A–C**, TNBS; **D–F**, DSS) demonstrate filling defects at the vessel bifurcations consistent with intussusceptive pillars. Because the intravascular injection of the casting media provided a cast of the lumen of the vessel, pillar formation appears as “holes” in the luminal cast. Note the regular pattern and morphology of the holes. Bar = 25 μm.

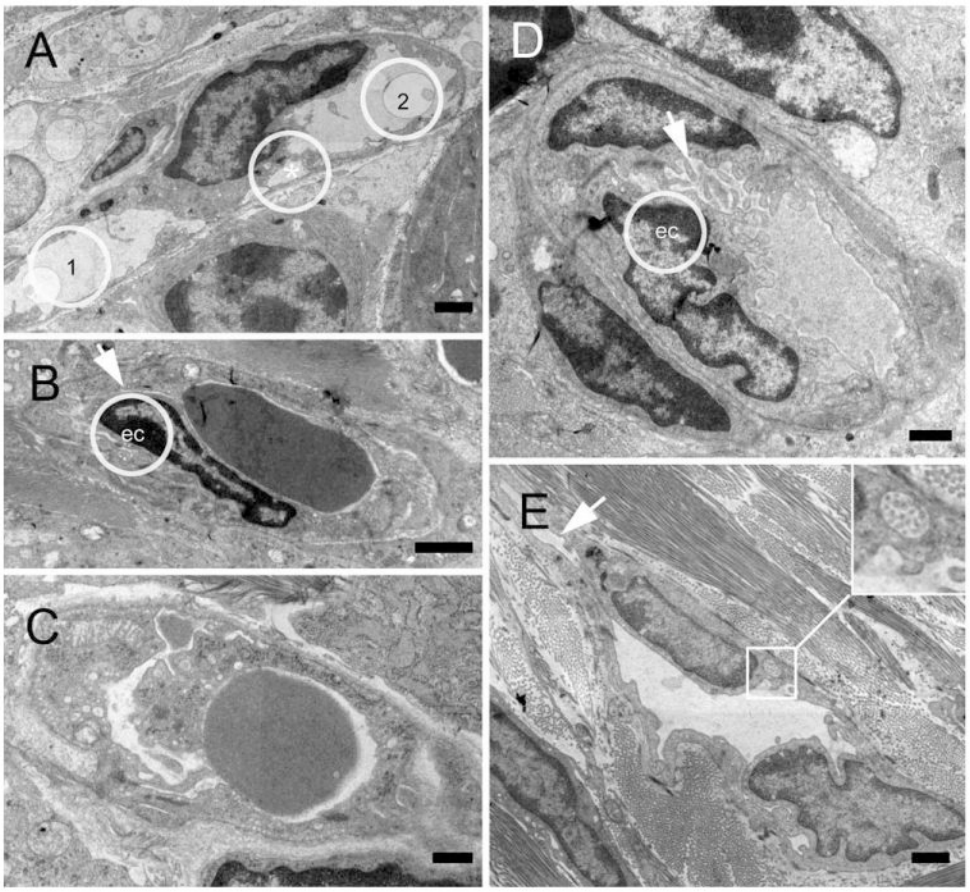

Fig. 6.

Transmission electron micrographs of intussusceptive angiogenesis features in the colon mucosal plexus 6 days after stimulation. (**A**) Pillar composed of endothelial cells dividing the original lumen into two lumens (1,2). Endothelial folds still separate two minor lumens (*). (**B–D**) Earlier stages of pillar formation with protrusion of endothelial cells (ec) separating newly formed lumens (arrows). (**E**) Vascular lining cells engulfing collagen fiber bundles (inset) indicate that nonendothelial cells participate in pillar formation and intussusceptive angiogenesis (Bar = 2 μm).